Modern Physics Letters B
Vol. 33, No. 17 (2019) 1950195 (15 pages)

DOI: 10.1142/S0217984919501951

Classifying superconductivity in compressed H_3S

E. F. Talantsev

M.N. Mikheev Institute of Metal Physics, Ural Branch,
Russian Academy of Sciences, 18, S. Kovalevskoy St.,
Ekaterinburg 620108, Russia
NANOTECH Centre, Ural Federal University,
19 Mira St., Ekaterinburg 620002, Russia
evgeny.talantsev@imp.uran.ru

Received 5 February 2019
Revised 20 March 2019
Accepted 27 March 2019
Published 3 June 2019

The discovery of high-temperature superconductivity in compressed H_3S by Drozdov and co-workers [A. Drozdov *et al.*, *Nature* **525** (2015) 73] heralded a new era in superconductivity. To date, the record transition temperature of $T_c = 260$ K stands with another hydrogen-rich compound, LaH_{10} [M. Somayazulu *et al.*, *Phys. Rev. Lett.* **122** (2019) 027001] which becomes superconducting at pressure of $P = 190$ GPa. Despite very intensive first-principle theoretical studies of hydrogen-rich compounds compressed to megabar level pressure, there is a very limited experimental dataset available for such materials. In this paper, we analyze the upper critical field, $B_{c2}(T)$, data of highly compressed H_3S reported by Mozaffari and co-workers [S. Mozaffari *et al.*, *LA-UR*-18-30460, doi:10.2172/1481108] by utilizing four different models of $B_{c2}(T)$. As the result, we find that the ratio of superconducting energy gap, $\Delta(0)$, to the Fermi energy, ε_F, in all considered scenarios is $0.03 < \Delta(0)/\varepsilon_F < 0.07$, with respective ratio of T_c to the Fermi temperature, T_F, $0.012 < T_c/T_F < 0.039$. These characterize H_3S as unconventional superconductor and places it on the same trend line in T_c versus T_F plot, where all unconventional superconductors are located.

Keywords: Hydrogen-rich superconducting compounds; upper critical field; unconventional superconductivity; high pressure; sulphur hydrides.

1. Introduction

Experimental discovery of a superconductivity above $T = 200$ K in highly compressed H_3S by Drozdov *et al.*[1] is one of the most fascinating confirmations of the Bardeen–Cooper–Schrieffer (BCS) theory[2] and the phonon-mediated pairing scenario which can sustain superconductivity at such high temperature.[3,4] Moreover, recent experimental results on another hydrogen-rich compound of LaH_{10} (Refs. 5 and 6), further showed that BCS electron–phonon pairing mechanism works at much

higher temperatures, and highest observed in experiment superconducting transition temperature, T_c, for LaH_{10} compound is $T_c = 260$ K.[6] Historical aspects of the discovery, including the astonishing theoretical prediction of Ashcroft,[7] and reviews of experimental and theoretical works in the field can be found elsewhere.[8–17]

Most theoretical works,[10,12,13,18–22] except, perhaps, the only work by Kaplan and Imry,[23] came to conclusion that H_3S is strong coupled superconductor with BCS ratio:

$$\frac{2 \cdot \Delta(0)}{k_B \cdot T_c} = \alpha = 4.5 - 4.7\,, \tag{1}$$

where $\Delta(0)$ is ground state superconducting energy gap, k_B is the Boltzmann constant. In contrast to this, our analysis[24] of experimental self-field critical current density, $J_c(\text{sf}, T)$ (reported by Drozdov and co-workers in Ref. 1), showed that the BCS ratio (Eq. (1)) for H_3S is more likely to be very close to the weak-coupling limit of 3.53, and we deduced value for $\Delta(0) = 28$ meV,[24,25] while many theoretical works came to predicted values in the range of $\Delta(0) = 40$–45 meV. Modern spectroscopic techniques have been applied to H_3S,[26] which confirmed theoretically calculated energy spectrum for energies above 70 meV.

In this paper, we analyze recently released experimental upper critical field, $B_{c2}(T)$, data[27] for highly compressed H_3S with the purpose of deducing the Fermi velocity, v_F, and Fermi energy, ε_F, for this material.

2. Description of Models

In the Ginzburg–Landau (GL) theory, the upper critical field is given by following expression:

$$B_{c2}(T) = \frac{\phi_0}{2 \cdot \pi \cdot \xi^2(T)}, \tag{2}$$

where $\phi_0 = 2.07 \cdot 10^{-15}$ Wb is flux quantum and $\xi(T)$ is the coherence length. There is a well-known BCS expression[2]

$$\xi(0) = \frac{\hbar \cdot v_F}{\pi \cdot \Delta(0)}, \tag{3}$$

where $\hbar = h/2\pi$ is reduced Planck constant and v_F is the Fermi velocity. Thus, from deduced $B_{c2}(0)$ and T_c and assumed α (Eq. (1)), one can calculate the Fermi velocity, v_F as

$$v_F = \frac{\pi}{2} \cdot \xi(0) \cdot \frac{\alpha \cdot k_B \cdot T_c}{\hbar}, \tag{4}$$

the Fermi energy, ε_F:

$$\varepsilon_F = \frac{m^*_{\text{eff}} \cdot v_F^2}{2}, \tag{5}$$

where m^*_{eff} is effective mass of charge carriers (for H_3S we used $m^*_{\text{eff}} = 2.76 \cdot m_e$ where m_e is electron mass (Ref. 10)), and the Fermi temperature, T_F:

$$T_F = \frac{\varepsilon_F}{k_B}. \tag{6}$$

One of conventional models to analyze $B_{c2}(T)$ was given by Werthamer–Helfand–Hohenberg (WHH)[28,29]:

$$\ln\left(\frac{T}{T_c(B=0)}\right) = \psi\left(\frac{1}{2}\right) - \psi\left(\frac{1}{2} + \frac{\hbar \cdot D \cdot B_{c2}(T)}{2 \cdot \phi_0 \cdot k_B \cdot T}\right), \tag{7}$$

where ψ is digamma function, D is the diffusion constant of the normal conducting electrons/holes, with two free fitting parameters of $T_c(B = 0)$ and D. This model is originated from the BCS theory.[2] Baumgartner *et al.*[30] proposed simple and accurate analytical expression for $B_{c2}(T)$ within WHH model

$$B_{c2}(T) = \frac{1}{0.693} \cdot \frac{\phi_0}{2 \cdot \pi \cdot \xi^2(0)} \cdot \left(\left(1 - \frac{T}{T_c}\right) - 0.153 \cdot \left(1 - \frac{T}{T_c}\right)^2 - 0.152 \cdot \left(1 - \frac{T}{T_c}\right)^4\right), \tag{8}$$

where $\xi(0)$ and $T_c \equiv T_c(B = 0)$ are two free fitting parameters. Equation (8) (Ref. 30) was developed as analytical tool for extrapolation on low temperature/high field region of $B_{c2}(T)$, because for many practical superconductors experimental conditions allow to measure only the high reduced temperatures ($T/T_c \geq 0.5$) and/or low applied magnetic fields ($B/B_{c2}(T = 0\ \text{K}) < 0.5$) part of the whole $B_{c2}(T)$ curve (it can be seen in Figs. 1–4, that this is the case for H_3S superconductor too). We note that Eq. (7) requires for the analysis reasonably rich raw $B_{c2}(T)$ dataset which distributes uniformly over the whole entire temperature range from very low temperatures up to T_c. In this regard, for many practical cases, Eq. (8) is a very good extrapolative analytical tool which alternates the application of initial Eq. (7). We will designate Eq. (8) as B-WHH model.

In addition to Eqs. (7) and (8), there are several analytical expressions which are in wide usage, too.[31–33] For instance, there are classical two-fluid Gorter–Casimir model[34]:

$$B_{c2}(T) = \frac{\phi_0}{2 \cdot \pi \cdot \xi^2(0)} \cdot \left(1 - \left(\frac{T}{T_c}\right)^2\right) \tag{9}$$

and Jones–Hulm–Chandrasekhar (JHC) model[35]:

$$B_{c2}(T) = \frac{\phi_0}{2 \cdot \pi \cdot \xi^2(0)} \cdot \left(\frac{1 - \left(\frac{T}{T_c}\right)^2}{1 + \left(\frac{T}{T_c}\right)^2}\right). \tag{10}$$

Equation (10) was also developed by Jones *et al.*[35] as one of low temperature/high field extrapolative tools which utilizes experimental $B_{c2}(T)$ datasets

recorded at relatively high reduced temperatures/low applied magnetic field. We need to note that if Eqs. (7) and (8) (Refs. 28–30) originated from the BCS theory, the JHC model (Eq. (10) (Ref. 35)) utilizes the GL theory.[36,37]

There is also a little-known equation from Gor'kov for $B_{c2}(T)$[38] which was referred by Gor'kov as a good analytical interpolative approximation over the whole temperature range:

$$B_{c2}(T) = B_c(T) \cdot \frac{\sqrt{2}}{1.77} \cdot \frac{\lambda(0)}{\xi(0)} \cdot \left(1.77 - 0.43 \cdot \left(\frac{T}{T_c}\right)^2 + 0.07 \cdot \left(\frac{T}{T_c}\right)^4\right), \quad (11)$$

where $B_c(T)$ is the thermodynamic critical field, and $\lambda(0)$ is the ground state London penetration depth. It is a well-known fact that Gor'kov showed[39] that GL theory[36,37] is the high-temperature limit of BCS theory.[2] Thus, Eq. (11) can be considered as a good alternative tool to analyze experimental $B_{c2}(T)$ data which accumulates advantages of both GL and BCS theories.

Equation (11) was re-written by Jones *et al.*[35] in following form:

$$B_{c2}(T) = \frac{1}{1.77} \cdot \frac{\phi_0}{2 \cdot \pi \cdot \xi^2(0)} \cdot \left(1.77 - 0.43 \cdot \left(\frac{T}{T_c}\right)^2 + 0.07 \cdot \left(\frac{T}{T_c}\right)^4\right) \cdot \left[1 - \left(\frac{T}{T_c}\right)^2\right], \quad (12)$$

where the expression in the square brackets is obviously two-fluid model of Gorter–Casimir (Eq. (9) (Ref. 35)). We will designate Eq. (12) as G model.

In this paper, we utilize Eq. (11) in a different way, to be oriented on the deriving fundamental parameters of superconductor, for instance, $\Delta(0)$, and thus, we reconsidered the square brackets substitution in Eq. (12), by general BCS theory approach, where all properties of superconductor originated from the superconducting energy gap, $\Delta(T)$.

Truly, if we take into account, the GL theory expressions:

$$B_{c2}(T) = \sqrt{2} \cdot \frac{\lambda(T)}{\xi(T)} \cdot B_c(T), \quad (13)$$

we can conclude that the Gor'kov's equation (Eq. (11)) means that

$$\kappa(T) = \frac{\lambda(T)}{\xi(T)} = \frac{1}{1.77} \cdot \frac{\lambda(0)}{\xi(0)} \cdot \left(1.77 - 0.43 \cdot \left(\frac{T}{T_c}\right)^2 + 0.07 \cdot \left(\frac{T}{T_c}\right)^4\right). \quad (14)$$

By utilizing another GL theory expression:

$$B_{c2}(T) = 2 \cdot \left(\frac{\lambda(T)}{\xi(T)}\right)^2 \cdot \frac{B_{c1}(T)}{\ln(\kappa(T)) + 0.5} = \left(\frac{\lambda(T)}{\xi(T)}\right)^2 \cdot \frac{\phi_0}{2 \cdot \pi \cdot \lambda^2(T)} = (\kappa(T))^2 \cdot \frac{\phi_0}{2 \cdot \pi \cdot \lambda^2(T)} \quad (15)$$

and BCS expression for $\lambda(T)$ for s-wave superconductor:

$$\lambda(T) = \frac{\lambda(0)}{\sqrt{1 - \frac{1}{2\cdot k_B \cdot T} \cdot \int_0^\infty \frac{d\varepsilon}{\cosh^2\left(\frac{\sqrt{\varepsilon^2+\Delta^2(T)}}{2\cdot k_B \cdot T}\right)}}}, \tag{16}$$

where the temperature-dependent superconducting gap $\Delta(T)$ equation can be taken from Gross *et al.*[40]:

$$\Delta(T) = \Delta(0) \cdot \tanh\left[\frac{\pi \cdot k_B \cdot T_c}{\Delta(0)} \cdot \sqrt{\eta \cdot \frac{\Delta C}{C} \cdot \left(\frac{T_c}{T} - 1\right)}\right], \tag{17}$$

where $\Delta C/C$ is the relative jump in electronic specific heat at T_c, and $\eta = 2/3$ for s-wave superconductors,[40] one can obtain expression for the temperature-dependent upper critical field:

$$B_{c2}(T) = \frac{\phi_0}{2 \cdot \pi \cdot \xi^2(0)} \cdot \left[\left(\frac{1.77 - 0.43 \cdot \left(\frac{T}{T_c}\right)^2 + 0.07 \cdot \left(\frac{T}{T_c}\right)^4}{1.77}\right)^2 \cdot \frac{1}{1 - \frac{1}{2\cdot k_B \cdot T} \cdot \int_0^\infty \frac{d\varepsilon}{\cosh^2\left(\frac{\sqrt{\varepsilon^2+\Delta^2(T)}}{2\cdot k_B \cdot T}\right)}}\right]. \tag{18}$$

Thus, four fundamental parameters of superconductor, i.e. $\xi(0)$, $\Delta(0)$, $\Delta C/C$ and T_c, can be deduced by fitting experimental $B_{c2}(T)$ data to Eq. (18). We need to clarify that $\xi(0)$ determines absolute value of $B_{c2}(0)$ amplitude, while $\Delta(0)$ and $\Delta C/C$ are deduced from the shape of $B_{c2}(T)$ curve (which is the part of Eq. (18) in square brackets).

In this paper, we fit experimental $B_{c2}(T)$ data for compressed sulfur hydride to Eqs. (8), (10), (12) and (18) by using nonlinear curve fitting in the ORIGIN plot package with the purpose to deduce/calculate fundamental superconducting parameters of this material.

3. Results and Discussions

There are several approaches to defining $B_{c2}(T)$ from experimental $R(T)$ curves. For instance, a given applied field can be defined as B_{c2} at the temperature of the onset of the superconducting transition (i.e. initial deviation from the normal state resistance, $R_{\rm norm}(T)$), or at the temperature of the 90%, 50%, or 10% fraction of $R_{\rm norm}(T)$, or it can be most rigorously defined at the zero resistance point, $R = 0\ \Omega$. Mozaffari *et al.*[27] in their Fig. 1(a) defined the upper critical field by two criteria:

(1) At the onset of superconducting transition, which we will designate as $B_{c2}(T)$ (in accordance with Mozaffari *et al.*[27] definition).

(2) At the zero-resistance point, which we will designate as $B_{c2,R=0}(T)$ for the clarity.

In Figs. 1–4, we show raw upper critical field data and data fits to four models:

Panel (a): B-WHH model[29] (Eq. (8));
Panel (b): JHC model[35] (Eq. (10));
Panel (c): G model[38] (Eq. (12));
Panel (d): this work model (Eq. (18)).

In Figs. 1 and 2, we show results for Sample #1 compressed at $P = 155$ GPa. In Figs. 3 and 4, we show results for Sample #2 compressed at $P = 160$ GPa. In Figs. 1 and 3, we analyzed $B_{c2,R=0}(T)$ data, and in Figs. 2 and 4, we analyzed $B_{c2}(T)$ data. Results of all fits are presented in Table 1.

In general (Figs. 1–4, Table 1), we can conclude that all four models provide good fit quality, R, and deduced values of T_c and $\xi(0)$ for all four models are in reasonable agreement with each other. The most interesting thing we found is that fits to Eq. (18) reveal for all four $B_{c2}(T)$ datasets the value for superconducting energy gap of $\Delta(0) = 25$–28 meV which all are in excellent agreement with the value we deduced by the analysis of critical current densities in H_3S in our previous work,[24,25] $\Delta(0) = 28$ meV. The latter was deduced for different H_3S sample[1] with $T_c = 203$ K, while in present work we analyzed data for samples with lower T_c.

All deduced $B_{c2}(0)$ values (Figs. 1–4) are well below Pauli limit of

$$B_p(0) = \frac{2 \cdot \Delta(0)}{g \cdot \mu_B} = 430 - 500\,T \gg B_{c2}(0), \tag{19}$$

where $g = 2$ and $\mu_B = \frac{e \cdot \hbar}{2 \cdot m_e}$ is the Bohr magneton.

Following Gor'kov's note,[41] Eq. (19) means that the mean-free path, l, of the electrons is large compared with the coherence length:

$$l \gg \xi(T) > \xi(0) \sim 2.5\,\text{nm}. \tag{20}$$

This is interesting result, if we take into account that H_3S is formed by chemical reaction which occurs within the diamond anvil volume:

$$3H_2S \rightarrow 2H_3S + S \tag{21}$$

and pure sulfur is always presented as post-reacted product in the studied sample.

However, Eq. (19) tells us that two phases, i.e. H_3S and S, are reasonably well separated from each other and there is a very low level of atomic disordering within superconducting H_3S phase, which has lattice parameter of $a = 0.3092$ nm.[42]

The next step of the analysis is the comparison of v_F, ε_F, T_F values calculated directly by Eq. (3) (because fits to Eq. (18) provide both required quantities, i.e. $\xi(0)$ and $\Delta(0)$) with v_F values calculated by Eq. (4) in assumption of two extreme coupling-strength scenarios of $\alpha = 3.53$ and $\alpha = 4.70$. Overall, deduced/calculated v_F for H_3S are in the range of $v_F = 2.0$–3.8×10^5 m/s which equals to v_F of nickel

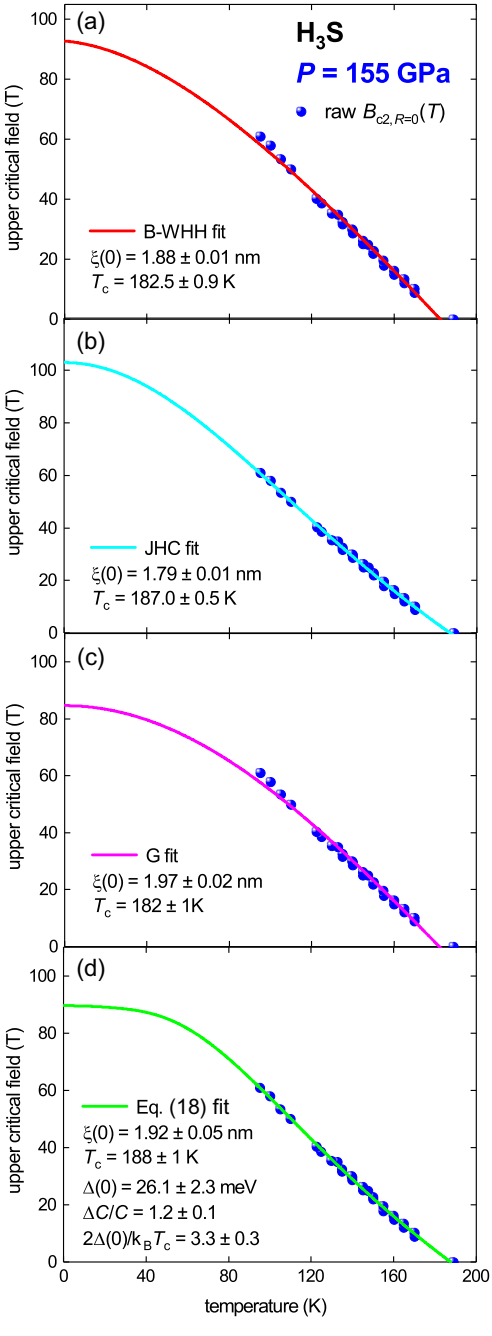

Fig. 1. (Color online) Superconducting upper critical field, $B_{c2,R=0}(T)$, data (blue) for compressed H_3S Sample #1 at pressure $P = 155$ GPa (raw data are from Ref. 27). (a) Fit to B-WHH model[29] (Eq. (8)), fit quality is $R = 0.9901$. (b) Fit to JHC model[35] (Eq. (10)), fit quality is $R = 0.9978$. (c) Fit to G model[38] (Eq. (12)), fit quality is $R = 0.9879$. (d) Fit to this work model (Eq. (18)); fit quality is $R = 0.9979$.

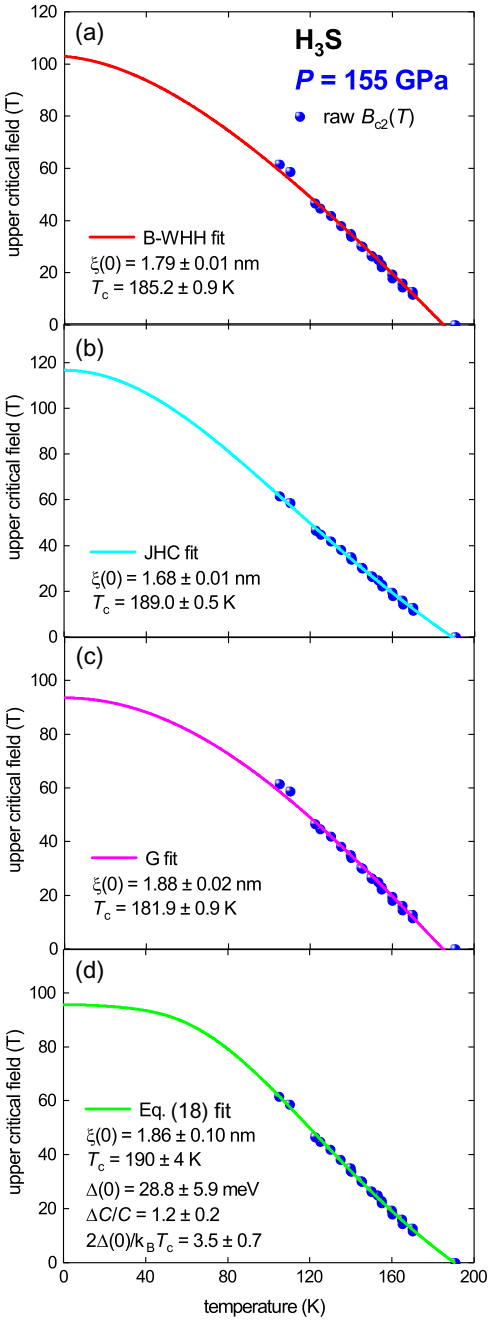

Fig. 2. (Color online) Superconducting upper critical field, $B_{c2}(T)$, data (blue) for compressed H_3S Sample #1 at pressure $P = 155$ GPa (raw data are from Ref. 27). (a) Fit to B-WHH model[29] (Eq. (8)), fit quality is $R = 0.990$. (b) Fit to JHC model[35] (Eq. (10)), fit quality is $R = 0.9978$. (c) Fit to G model[38] (Eq. (12)), fit quality is $R = 0.9886$. (d) Fit to this work model (Eq. (18)); fit quality is $R = 0.9981$.

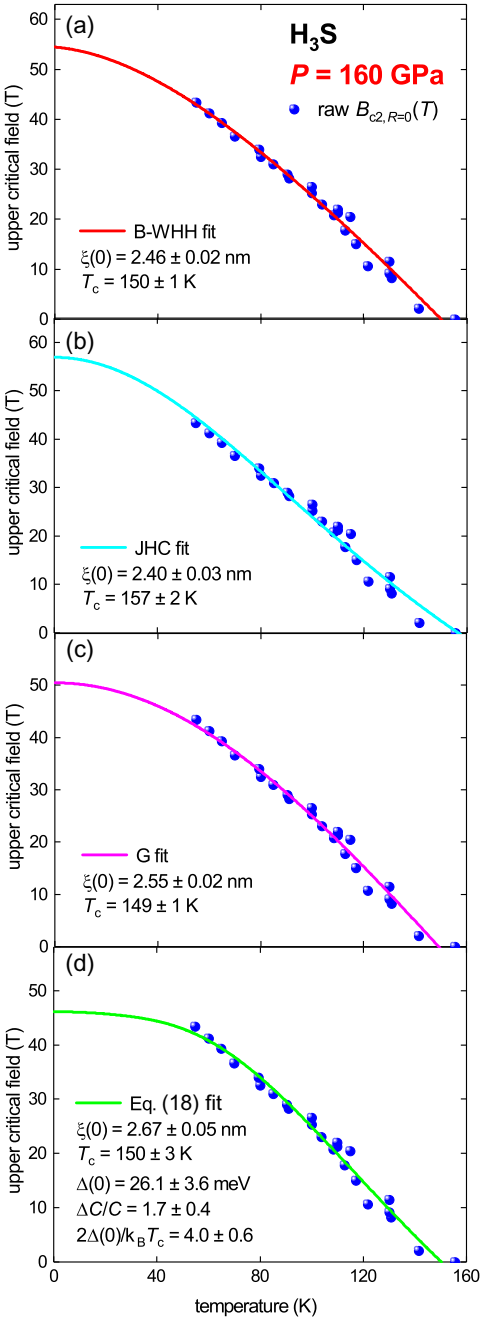

Fig. 3. (Color online) Superconducting upper critical field, $B_{c2,R=0}(T)$, data (blue) for compressed H_3S Sample #2 at pressure $P = 160$ GPa (raw data are from Ref. 27). (a) Fit to B-WHH model[29] (Eq. (8)), fit quality is $R = 0.9832$. (b) Fit to JHC model[35] (Eq. (10)), fit quality is $R = 0.9785$. (c) Fit to G model[38] (Eq. (12)), fit quality is $R = 0.9827$. (d) Fit to this work model (Eq. (18)), fit quality is $R = 0.9832$.

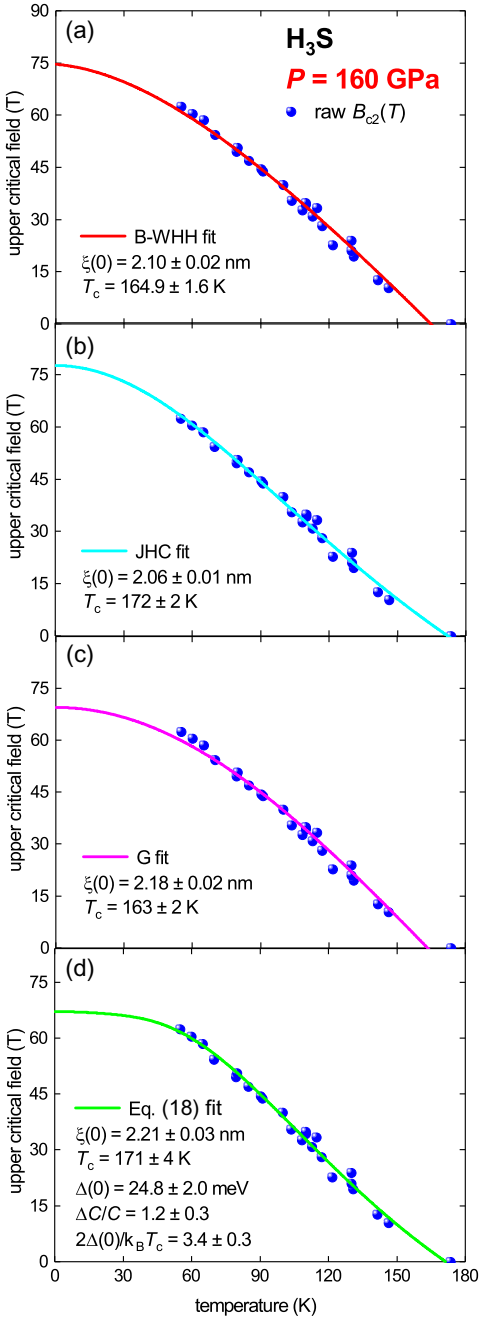

Fig. 4. (Color online) Superconducting upper critical field, $B_{c2}(T)$, data (blue) for compressed H_3S Sample #2 at pressure $P = 160$ GPa (raw data are from Ref. 27). (a) Fit to B-WHH model[29] (Eq. (8)), fit quality is $R = 0.9850$. (b) Fit to JHC model[35] (Eq. (10)), fit quality is $R = 0.9908$. (c) Fit to G model[38] (Eq. (12)), fit quality is $R = 0.9806$. (d) Fit to this work model (Eq. (18)); fit quality is $R = 0.9914$.

Table 1. Deduced parameters for H_3S superconductor. We assumed that electron effective mass in H_3S is $m_{\text{eff}} = 2.76\ m_e$.[10]

Pressure (GPa)	Raw data	Model	Deduced T_c (K)	Deduced $\xi(0)$ (nm)	Assumed/ deduced $\frac{2\cdot\Delta(0)}{k_B\cdot T_c}$	$\Delta C/C$	v_F (10^5 m/s)	$\Delta(0)$ (meV)	ε_F (eV)	$\Delta(0)/\varepsilon_F$	T_F (10^3 K)	T_c/T_F
160	$B_{c2,R=0}(T)$	B-WHH	150 ± 1	2.46 ± 0.02	3.53		2.68 ± 0.03	22.8 ± 0.2	0.56 ± 0.01	0.040 ± 0.001	6.5 ± 0.2	0.023 ± 0.001
					4.70		3.57 ± 0.04	30.4 ± 0.04	1.00 ± 0.02	0.030 ± 0.001	11.6 ± 0.4	0.013 ± 0.001
		JHC	157 ± 2	2.40 ± 0.03	3.53		2.74 ± 0.03	23.9 ± 0.4	0.59 ± 0.03	0.041 ± 0.002	6.8 ± 0.2	0.023 ± 0.001
					4.70		3.65 ± 0.05	31.8 ± 0.4	1.04 ± 0.02	0.030 ± 0.002	12.1 ± 0.5	0.013 ± 0.001
		G	149 ± 1	2.55 ± 0.02	3.53		2.76 ± 0.03	22.7 ± 0.2	0.60 ± 0.01	0.038 ± 0.002	6.9 ± 0.2	0.021 ± 0.001
					4.70		3.68 ± 0.04	30.2 ± 0.3	1.06 ± 0.02	0.028 ± 0.001	12.3 ± 0.5	0.012 ± 0.001
		Eq. (18)	150 ± 3	2.67 ± 0.05	4.0 ± 0.6	1.7 ± 0.4	3.33 ± 0.45	26.1 ± 3.6	0.87 ± 0.12	0.030 ± 0.004	10.1 ± 1.4	0.015 ± 0.002
	$B_{c2}(T)$	B-WHH	165 ± 2	2.10 ± 0.02	3.53		2.51 ± 0.03	25.1 ± 0.3	0.50 ± 0.01	0.051 ± 0.002	5.8 ± 0.2	0.029 ± 0.001
					4.70		3.35 ± 0.03	33.4 ± 0.3	0.88 ± 0.02	0.038 ± 0.002	10.2 ± 0.2	0.016 ± 0.001
		JHC	172 ± 2	2.06 ± 0.01	3.53		2.57 ± 0.03	26.2 ± 0.3	0.52 ± 0.01	0.050 ± 0.002	6.0 ± 0.2	0.029 ± 0.001
					4.70		3.42 ± 0.03	34.8 ± 0.3	0.92 ± 0.02	0.038 ± 0.001	10.7 ± 0.2	0.016 ± 0.001
		G	163 ± 2	2.18 ± 0.02	3.53		2.58 ± 0.05	24.8 ± 0.3	0.52 ± 0.02	0.048 ± 0.002	6.0 ± 0.2	0.027 ± 0.001
					4.70		3.43 ± 0.07	33.0 ± 0.3	0.92 ± 0.05	0.036 ± 0.002	10.7 ± 0.2	0.015 ± 0.001
		Eq. (18)	171 ± 4	2.21 ± 0.03	3.4 ± 0.3	1.2 ± 0.3	2.6 ± 0.3	24.8 ± 2.0	0.54 ± 0.06	0.046 ± 0.005	6.3 ± 0.5	0.027 ± 0.003
155	$B_{c2,R=0}(T)$	B-WHH	182.5 ± 0.9	1.88 ± 0.01	3.53		2.50 ± 0.03	27.8 ± 0.1	0.49 ± 0.01	0.057 ± 0.002	5.7 ± 0.2	0.032 ± 0.002
					4.70		3.32 ± 0.02	37.0 ± 0.2	0.87 ± 0.01	0.043 ± 0.001	10.0 ± 0.2	0.018 ± 0.001
		JHC	187.0 ± 0.5	1.79 ± 0.01	3.53		2.43 ± 0.01	28.4 ± 0.1	0.46 ± 0.01	0.062 ± 0.001	5.4 ± 0.1	0.035 ± 0.001
					4.70		3.23 ± 0.01	37.9 ± 0.1	0.82 ± 0.01	0.046 ± 0.001	9.5 ± 0.1	0.020 ± 0.001
		G	182 ± 1	1.97 ± 0.02	3.53		2.61 ± 0.01	27.7 ± 0.1	0.53 ± 0.01	0.052 ± 0.001	6.2 ± 0.1	0.030 ± 0.001
					4.70		3.47 ± 0.01	36.9 ± 0.1	0.94 ± 0.01	0.039 ± 0.001	11.0 ± 0.2	0.017 ± 0.001
		Eq. (18)	188 ± 1	1.92 ± 0.05	3.3 ± 0.3	1.2 ± 0.1	2.4 ± 0.2	26.1 ± 2.3	0.44 ± 0.05	0.059 ± 0.006	5.0 ± 0.5	0.037 ± 0.004
	$B_{c2}(T)$	B-WHH	185.2 ± 0.9	1.79 ± 0.01	3.53		2.40 ± 0.01	28.2 ± 0.1	0.45 ± 0.01	0.062 ± 0.001	5.3 ± 0.1	0.035 ± 0.001
					4.70		3.20 ± 0.01	37.5 ± 0.1	0.80 ± 0.02	0.047 ± 0.002	9.3 ± 0.2	0.020 ± 0.001
		JHC	189.0 ± 0.5	1.68 ± 0.01	3.53		2.30 ± 0.01	28.7 ± 0.1	0.42 ± 0.01	0.069 ± 0.002	4.8 ± 0.2	0.039 ± 0.001
					4.70		2.07 ± 0.01	38.3 ± 0.1	0.74 ± 0.02	0.052 ± 0.002	8.6 ± 0.2	0.022 ± 0.001
		G	181.9 ± 0.9	1.97 ± 0.02	3.53		2.48 ± 0.02	27.7 ± 0.1	0.48 ± 0.01	0.057 ± 0.002	5.6 ± 0.3	0.033 ± 0.002
					4.70		3.30 ± 0.02	36.8 ± 0.1	0.85 ± 0.02	0.043 ± 0.002	9.9 ± 0.3	0.018 ± 0.001
		Eq. (18)	190 ± 4	1.86 ± 0.10	3.5 ± 0.7	1.2 ± 0.2	2.6 ± 0.4	28.8 ± 5.9	0.51 ± 0.09	0.056 ± 0.009	6.0 ± 1.0	0.032 ± 0.006

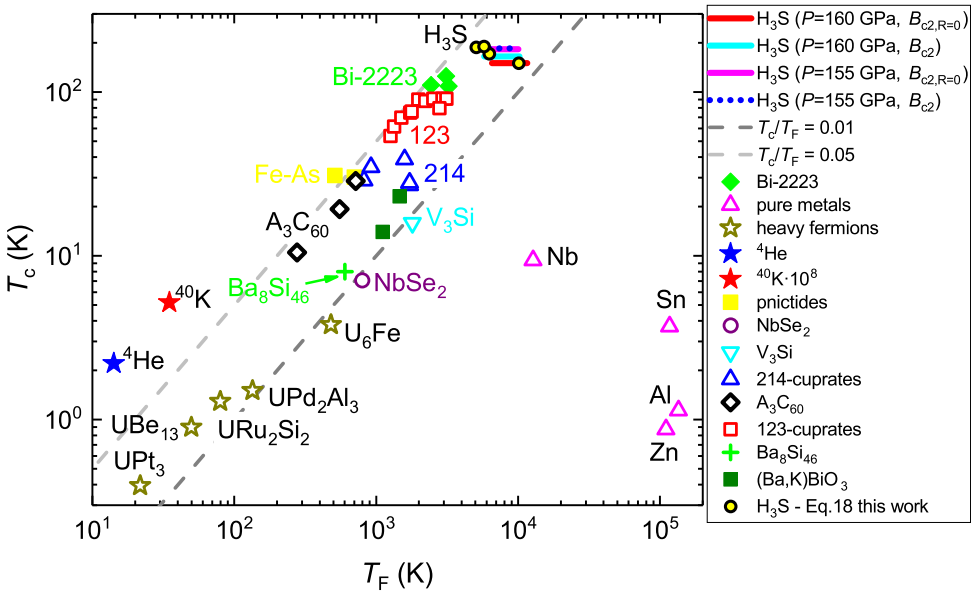

Fig. 5. (Color online) A plot of T_c versus T_F obtained for most representative superconducting families. Data was taken from Uemura,[46] Ye *et al.*,[47] Qian *et al.*[48] and Hashimoto *et al.*[49]

and cobalt at normal conditions[43] and is approximately equal to the universal nodal Fermi velocity of the superconducting cuprates.[44]

Examination of the values in Table 1 leaded us to three important findings:

1. The ratio of the superconducting energy gap, $\Delta(0)$, to the Fermi energy, ε_F, in all considered scenarios (including direct deduction by Eq. (18)) is within interval of $0.03 < \Delta(0)/\varepsilon_F < 0.07$. These values characterize H_3S material as an unconventional superconductor, by illustration, conventional niobium, Nb, has the ratio which is at least two orders of magnitude lower, i.e. $\Delta(0)/\varepsilon_F = 3 \cdot 10^{-4}$.[45]
2. The most straightforward way to see our conclusion that H_3S is unconventional superconductor is to add T_c and T_F data for H_3S on the plot of T_c versus T_F where other superconductors are shown. In this plot (Fig. 5) (data in Fig. 5 were adopted from Uemura,[46] Ye *et al.*,[47] Qian *et al.*,[48] and Hashimoto *et al.*[49]) all unconventional superconductors are located within a narrow band of $0.01 < T_c/T_F < 0.05$. We note that Uemura[46] stated that there is the upper limit for $T_c/T_F = 0.05$ for all known superconductors. In all considered scenarios, H_3S has ratios within interval of $0.012 < T_c/T_F < 0.039$ (Fig. 5 and Table 1). It is clearly visible in Fig. 5 that H_3S lies in the same band as all unconventional superconductors, particularly heavy fermions and falls just above Bi-2223 phase in the plot. In this regard, H_3S is the material which is located together with the majority of others unconventional superconductors placed.

3. We also can see that despite very different assumptions and varieties of the upper critical field data definition, the Fermi velocity is within reasonably narrow interval of $v_F = 2.0$–$3.8 \cdot 10^5$ m/s. This value is about two times lower than v_F of alkali metals at normal conditions[43,45] and it approximately equals to the universal nodal Fermi velocity of the superconducting cuprates.[44] This is another manifestation that H_3S should be classified as unconventional superconductor.

Even though the original paper from Drozdov *et al.*[1] stated that H_3S is conventional superconductor, and this point of view was very quickly and widely accepted by the scientific community,[3] we must note that at that time there were no available experimental data which supported this point of view. One of prerequisites of phonon-mediated mechanism in H_3S is the strong-coupling electron–phonon interaction (references on original papers can be found in Ref. 13), which we cannot confirm neither by the analysis of experimental critical current densities,[24,25] nor by the analysis of experimental upper critical field data presented herein. Instead our analysis gives clear evidence that H_3S is weak-coupled superconductor, with the ratio:

$$3.3 \pm 0.3 < \frac{2 \cdot \Delta(0)}{k_B \cdot T_c} < 4.0 \pm 0.6 \tag{22}$$

and average value of

$$\frac{2 \cdot \Delta(0)}{k_B \cdot T_c} = 3.55 \pm 0.31 \tag{23}$$

which is remarkably closed to weak-coupling limit of BCS theory of 3.53 (Ref. 2) and to the value predicted by recent theoretical model developed by Kaplan and Imry of 3.50.[23]

Average absolute value of the ground state superconducting energy gap is

$$\Delta(0) = 26.5 \pm 1.7 \text{ meV}. \tag{24}$$

This value is in a very good agreement with $\Delta(0) = 27.8$ meV which we deduced in our previous paper by the analysis of critical current density in H_3S (Refs. 24 and 25) for sample with $T_c = 203$ K.

4. Conclusion

In this paper, we analyzed the upper critical field data for compressed H_3S which were recently released by Los Alamos National Laboratory.[27] Result of our analysis showed that compressed H_3S should be classified as another member of unconventional superconductor family. Very recently Somayazulu *et al.*[6] reported that another hydrogen-rich compound LaH_{10} becomes superconducting at even higher temperature of $T = 260$ K, hence it will be a great interest to analyze the self-field critical current density data, $J_c(\text{sf},T)$,[50,51] the lower critical field data, $B_{c1}(T)$,[33,51] or the upper critical field data $B_{c2}(T)$ by the models used in the paper herein.

Acknowledgments

Author thanks two anonymous reviewers for helpful comments that lead to advance the paper. Author also thanks Mr. Ratu Mataira-Cole and Dr. Stuart Wimbush (Victoria University of Wellington, New Zealand) for reading, commenting and editing the paper, Dr. Daniel Kaplan (Weizmann Institute of Science, Israel) for the pointing out Ref. 23, and Prof. Jorge Hirsch (The University of California San Diego, USA) for the support.

The research was carried out within the state assignment of Minobrnauki of Russia (theme "Pressure" No. AAAA-A18-118020190104-3), supported in part by Act 211 Government of the Russian Federation, Contract No. 02.A03.21.0006.

References

1. A. P. Drozdov, M. I. Eremets, I. A. Troyan, V. Ksenofontov and S. I. Shylin, *Nature* **525** (2015) 73.
2. J. Bardeen, L. N. Cooper and J. R. Schrieffer, *Phys. Rev.* **108** (1957) 1175.
3. I. I. Mazin, *Nature* **525** (2015) 40.
4. N. Bernstein, C. S. Hellberg, M. D. Johannes, I. I. Mazin and M. J. Mehl, *Phys. Rev. B* **91** (2015) 060511.
5. A. P. Drozdov, V. S. Minkov, S. P. Besedin, P. P. Kong, M. A. Kuzovnikov, D. A. Knyazev and M. I. Eremets, arXiv:1808.07039.
6. M. Somayazulu, M. Ahart, A. K. Mishra, Z. M. Geballe, M. Baldini, Y. Meng, V. V. Struzhkin and R. J. Hemley, *Phys. Rev. Lett.* **122** (2019) 027001.
7. N. W. Ashcroft, *Phys. Rev. Lett.* **21** (1968) 1748.
8. M. I. Eremets and A. P. Drozdov, *Phys.-Usp.* **59** (2016) 1154.
9. I. Troyan *et al.*, *Science* **351** (2016) 1303.
10. A. P. Durajski, *Sci. Rep.* **6** (2016) 38570.
11. M. Einaga *et al.*, *Jpn. J. Appl. Phys.* **56** (2017) 05FA13.
12. H. Liu, I. I. Naumov, R. Hoffmann, N. W. Ashcroft and R. J. Hemley, *Proc. Natl. Acad. Sci. USA* **114** (2017) 6990.
13. L. P. Gor'kov and V. Z. Kresin, *Rev. Mod. Phys.* **90** (2018) 011001.
14. B. Liu *et al.*, *Phys. Rev. B* **98** (2018) 174101.
15. A. P. Durajski and R. Szczçśniak, *J. Chem. Phys.* **149** (2018) 074101.
16. Y. Yao and J. S. Tse, *Chem. Eur. J.* **24** (2018) 1769.
17. K. Shimizu *et al.*, *Physica C* **552** (2018) 27.
18. E. J. Nicol and J. P. Carbotte, *Phys. Rev. B* **91** (2015) 220507(R).
19. I. Errea *et al.*, *Phys. Rev. Lett.* **114** (2015) 157004.
20. T. Jarlborg and A. Bianconi, *Sci. Rep.* **6** (2016) 24816.
21. A. P. Durajski and R. Szczesniak, arXiv:1609.06079.
22. A. P. Durajski, R. Szczçśniak and L. Pietronero, *Ann. Phys.* **528** (2016) 358.
23. D. Kaplan and Y. Imry, *Proc. Natl. Acad. Sci. USA* **115** (2018) 5709.
24. E. F. Talantsev, W. P. Crump, J. G. Storey and J. L. Tallon, *Ann. Phys.* **529** (2017) 1600390.
25. E. F. Talantsev, W. P. Crump and J. L. Tallon, *Ann. Phys.* **529** (2017) 1700197.
26. F. Capitani *et al.*, *Nat. Phys.* **13** (2017) 859.
27. S. Mozaffari *et al.*, Los Alamos National Laboratory, Report LA-UR-18-30460 (2018); 10.2172/1481108.
28. E. Helfand and N. R. Werthamer, *Phys. Rev.* **147** (1966) 288.

29. N. R. Werthamer, E. Helfand and P. C. Hohenberg, *Phys. Rev.* **147** (1966) 295.
30. T. Baumgartner, M. Eisterer, H. W. Weber, R. Fluekiger, C. Scheuerlein and L. Bottura, *Supercond. Sci. Technol.* **27** (2014) 015005.
31. F. Yuan *et al.*, *New J. Phys.* **20** (2018) 093012.
32. B. Pal *et al.*, *Supercond. Sci. Technol.* **32** (2019) 015009.
33. E. F. Talantsev, W. P. Crump, J. O. Island, Y. Xing, Y. Sun, J. Wang and J. L. Tallon, *2D Mater.* **4** (2017) 025072.
34. C. J. Gorter and H. Casimir, *Physica* **1** (1934) 306.
35. C. K. Jones, J. K. Hulm and B. S. Chandrasekhar, *Rev. Mod. Phys.* **36** (1964) 74.
36. V. L. Ginzburg and L. D. Landau, *Zh. Eksp. Teor. Fiz.* **20** (1950) 1064.
37. P. P. Poole, H. A. Farach, R. J. Creswick and R. Prozorov, *Superconductivity*, Chap. 6, 2nd edn. (London, UK, 2007).
38. L. P. Gor'kov, *Sov. Phys. JETP* **10** (1960) 593.
39. L. P. Gor'kov, *Sov. Phys. JETP* **9** (1959) 1364.
40. F. Gross, B. S. Chandrasekhar, D. Einzel, K. Andres, P. J. Hirschfeld, H. R. Ott, J. Beuers, Z. Fisk and J. L. Smith, *Z. Phys. B: Condens. Matter* **64** (1986) 175.
41. L. P. Gor'kov, *Sov. Phys. JETP* **17** (1963) 518.
42. M. Einaga *et al.*, *Nat. Phys.* **12** (2016) 835.
43. D. Gall, *J. Appl. Phys.* **119** (2016) 085101.
44. X. J. Zhou *et al.*, *Nature* **423** (2003) 398.
45. N. W. Aschroft and N. D. Mermin, *Solid State Physics* (Harcourt College Publishing, 1976), ISBN: 0030839939.
46. Y. J. Uemura, *J. Phys.: Condens. Matter* **16** (2004) S4515.
47. J. T. Ye, Y. J. Zhang, R. Akashi, M. S. Bahramy, R. Arita and Y. Iwasa, *Science* **338** (2012) 1193.
48. T. Qian *et al.*, *Phys. Rev. Lett.* **106** (2001) 187001.
49. K. Hashimoto *et al.*, *Science* **336** (2012) 1554.
50. E. F. Talantsev and J. L. Tallon, *Nat. Commun.* **6** (2015) 7820.
51. E. F. Talantsev, *Mod. Phys. Lett. B* **32** (2018) 1850114.